JOURNAL OF APPLIED ELECTROCHEMISTRY 10 (1980) 669–675

Kinetics of coloration of anodic electrochromic films of $WO_3 \cdot H_2O$

C. SUNSERI, F. DI QUARTO, A. DI PAOLA

Istituto di Ingegneria Chimica, University of Palermo, Italy

Received 10 October 1979

Polycrystalline layers of $WO_3 \cdot H_2O$ are obtained by anodization of tungsten in 1 N H_2SO_4 at 70° C. The cathodic reduction of these layers in acid solutions causes the formation of blue $WO_{3-x} \cdot H_2O$ ($0 < x \leqslant 0.12$) oxides. The kinetics of coloration are investigated by galvanostatic and potentiostatic techniques. The experimental results are compared with the theoretical data obtained by solving the diffusion equation for a constant flow of oxygen vacancies and for a time-dependent surface vacancy concentration. Except in the initial stage of coloration, the process controlling rate can be ascribed to the diffusion of oxygen vacancies from the oxide–electrolyte interface into the bulk of the layers. At low vacancy concentration, a barrier-limited proton transfer across the oxide–electrolyte interface seems to determine the kinetics of coloration.

1. Introduction

The challenge to develop new passive display devices has stimulated extensive investigation of those materials which exhibit the electrochromic effect, i.e. a reversible colour change induced by an electric field. Thus the electrochromic properties of WO_3 have been widely investigated [1–8]. It has been proposed that coloration of these films occurs with the formation of tungsten bronzes, M_xWO_3, according to the following reaction:

$$WO_3 + xM^{z+} + zxe = \underset{\text{(blue)}}{M_xWO_3} \qquad (1)$$

where M^{z+} is usually hydrogen, or other monovalent ions, e.g. Li^+, Na^+, Ag^+. In amorphous films of M_xWO_3 the optical absorption which produces the blue colour has been attributed to intervalence transitions, $W^{5+} \rightarrow W^{6+}$ [9], or small polaron transitions [10]. In polycrystalline WO_3 films, other studies [11] have suggested that the blue coloration is due to (a) conduction electron intraband transitions at high x, and (b) transitions from donor states to the conduction band at low x.

The electrochromic effect in polycrystalline $WO_3 \cdot H_2O$ anodic films has been also studied [12]. In this case the coloration takes place with the formation of $WO_{3-x} \cdot H_2O$ according to the reaction:

$$\underset{\text{(yellow-green)}}{WO_3 \cdot H_2O} + 2xH^+ + 2xe = \underset{\text{(blue)}}{WO_{3-x} \cdot H_2O} + xH_2 \qquad (0 < x \leqslant 0.12). \qquad (2)$$

The blue coloration has been attributed to the formation of F or F^+ centres in oxygen ion vacancies.

The knowledge of the rate-determining step (r.d.s.) of the electrochromic process allows the determination of the minimum obtainable write–erase time which is of technological interest. In fact, as known [1, 6, 13], some of the fundamental requirements which must be satisfied by electrochromic materials for their application in display devices are: (a) fast response, (b) good perceived contrast, (c) chemical stability.

Several hypotheses were put forward by different authors as to the r.d.s. of the process of coloration.

Crandall and Faughnan [14] proposed that at low voltages the kinetics of coloration of WO_3 amorphous films are controlled by the proton transport across the WO_3/electrolyte interface. This mechanism explains the observed decay of the coloration current with time as due to an increasing back-e.m.f. determined by the

0021–891X/80/050669–07$02.70/0

change of the chemical potential of hydrogen in H_xWO_3. The same model was assumed by Mohapatra [15] for the insertion of Li^+ in WO_3.

With increasing applied voltages a breakdown of this model was found and the proton diffusion in solution was proposed as the r.d.s. This last r.d.s. was also proposed by Chang *et al.* [16] to explain the observed dependence of the current i on time t, ($i \propto t^{-1/2}$) in the coloring process.

Reichmann and Bard [17] observed that the coloring process is faster at a WO_3 anodic film compared to a WO_3 evaporated film. This different kinetic behaviour was attributed to the different porosity and water content of these two films. By a detailed analysis of the current–time curves the authors concluded that a mass transfer process inside the film is the r.d.s. in the region where the current decays with a $t^{-1/2}$ dependence. The deviations at shorter and longer times were attributed to other mechanisms.

Green *et al.* [18], assuming that mass transport through WO_3 r.f. sputtered films was the r.d.s., calculated the optimum film thickness consistent with obtaining a high perceived contrast in a very short time ($t = 0.5$ s).

In the present paper the coloring process at $WO_3 \cdot H_2O$ anodic films is analysed. To elucidate the r.d.s., a model is proposed which involves oxygen vacancy diffusion inside the film. This model is supported by the experimental data obtained by galvanostatic and potentiostatic measurements.

2. Experimental

The electrodes were prepared by anodization of spectrographically pure tungsten sheets 0.1 mm thick. They were electropolished in NaOH 15 wt% at room temperature, rinsed with distilled water and dried in a nitrogen stream.

The anodization was performed in 1 N H_2SO_4 at 70° C, at a constant current density of 8 mA cm^{-2}. The current was supplied by a Keithley Model 227 constant current source. The duration of the anodization was always about 1 h so that anodic oxide layers of comparable weight and thickness were obtained.

The kinetics of coloration were investigated by inserting the oxide covered electrodes into an electrochemical cell containing 1 N H_2SO_4 solution at 25 ± 1° C. The electrode potential was measured with respect to a Hg/Hg_2SO_4 (1 N H_2SO_4) reference electrode by a Keithley Model 610 C electrometer.

An Amel Model 552 potentiostat was employed in the potentiostatic measurements: both the coloration current and the circulated electrical charge were simultaneously recorded by a Hewlett-Packard Model 7402 A oscillographic recorder. The coulometric measurements were carried out by a Amel Model 731 digital integrator.

The solutions were prepared from AR grade reagents and distilled water. To de-aerate the solution, nitrogen was slowly bubbled both before and during the colouring process.

Film thicknesses of about 1 μm were estimated by weight measurements and assuming a $WO_3 \cdot H_2O$ density of 5.5 g cm^{-3} [19].

3. Results and discussion

By anodization of tungsten in 1 N H_2SO_4 at 70° C, polycrystalline films of $WO_3 \cdot H_2O$ are obtained. The anodic charging curves and X-ray analysis have been reported in previous papers [12, 20].

The coloration of $WO_3 \cdot H_2O$ films has been attributed to the injection and trapping of electrons in oxygen ion vacancies $O\square^{\cdot\cdot}$ [12]. Vacancies are formed at the oxide–electrolyte interface according to the reaction:

$$WO_3 \cdot H_2O + 2xH^+ = xO\square^{\cdot\cdot} \quad (\text{in } WO_3 \cdot H_2O) + xH_2O \qquad (3)$$

They then diffuse in the bulk of the oxide layer where they capture electrons injected from the oxide–metal interface:

$$xO\square^{\cdot\cdot} \ (\text{in } WO_3 \cdot H_2O) + 2xe = WO_{3-x} \cdot H_2O \qquad (4)$$

the overall reaction occurs according to Equation 2.

3.1. *Galvanostatic measurements*

During the cathodic process the oxide colour changed from the initial yellow-green to the final deep blue. At the end of the experiments the electrodes were always covered by hydrogen bubbles.

At electrode potentials less negative than the hydrogen evolution potential the efficiency of vacancy injection is assumed to be one, i.e. the presence of reducible impurities in the electrolyte is neglected.

Moreover the essentially electronic conductivity of the hydrated tungsten oxide [21, 22] (especially with increasing vacancy concentration) and the narrow concentration range analysed support the following assumptions:

(a) a negligible contribution by electrical migration to vacancy transport through the oxide layer;

(b) a constant vacancy diffusion coefficient D independent of the concentration.

With these assumptions the vacancy concentration at distance y and at time t can be obtained by solving the time-dependent Fick's equation with the following initial and boundary conditions:

$$c = 0 \qquad t = 0 \qquad 0 \leqslant y \leqslant l$$

$$D\frac{\partial c}{\partial y} = \frac{i}{zF} = \text{const.} \qquad t > 0 \qquad y = l$$

$$D\frac{\partial c}{\partial y} = 0 \qquad t > 0 \qquad y = 0$$

Then we obtain [18, 23]:

$$c(y,t) = \frac{i}{zF}\frac{t}{l} + \frac{i}{zF}\frac{1}{D}\left[\frac{3y^2 - 1_l^2}{6l^2} - \frac{2}{\pi^2}\sum_{n=1}^{\infty}\frac{(-1)^n}{n^2} \times \exp\left(-\pi^2 n^2 \frac{Dt}{l^2}\right)\cos\left(\frac{n\pi y}{l}\right)\right] \qquad (5)$$

where $c(y, t)$ is the vacancy volume concentration, i the current density and l the film thickness ($y = 0$ at oxide–metal interface).

Fig. 1 shows the potential versus time curves for different current densities. After an initial inflection point the electrode potential decreases monotonically until a quasi steady-state value (not shown in figure) is obtained. This value depends on the applied current density but it is always greater than 1 V.

In Table 1 the electrode potential measured at different current densities and the corresponding surface vacancy concentration are reported. The concentration values were obtained by determining at different current densities the time required to reach the same potential and then inserting the i, t values into Equation 5. A diffusion layer thickness of about 0.1 μm was assumed in Equations 5 and 8 (see below) since the value of 1 μm (determined by weight) was considered to be unreliable, since the SEMs of the layers show a porous structure outside a barrier film [20]. A one-dimensional material flow is assumed inside the barrier film (about 0.05 μm thick), while both morphology and pore size suggest that the material flow along the pores should not be neglected. Therefore a virtual pore-free layer 0.05 μm thick is assumed to be equivalent to the porous layer. This assumption is supported by the experimental results. Clearly, the same diffusion layer thickness could be obtained by weight data assuming a surface ten times greater than the geometrical one. A diffusion coefficient of 5×10^{-10} cm^2 s^{-1} was determined by a trial and error method involving Equations 5 and 8.

Table 1 shows that, at every electrode potential the x values are practically independent of the applied current density. Then by Equation 5 we can obtain the surface vacancy concentration which determines the electrode potential.

Moreover the reversible potential of a non-stoichiometric electrode as function of the composition can be expressed, according to Crandall *et al.* [24] by the following equation obtained by a statistical mechanical analysis:

$$V = a + bx - n\frac{RT}{zF}\ln\left(\frac{x}{1-x}\right) \qquad (6)$$

where x is the surface vacancy concentration, a and b are constants, and n is a spatial correlation factor which can have the value of either one, if a close spatial correlation exists between electrons and oxygen vacancies, or two in absence of correlation.

In Fig. 2 Equation 6 is plotted using the experimental electrode potential values and the surface vacancy concentration obtained from Table 1. The straight-line behaviour over a wide range of electrode potentials supports the previous assumptions. A good fitting of the experimental data is possible using $n = 1$ as well as $n = 2$, however the high values of the static and optical dielectric constant of the WO_3 matrix suggest a partial

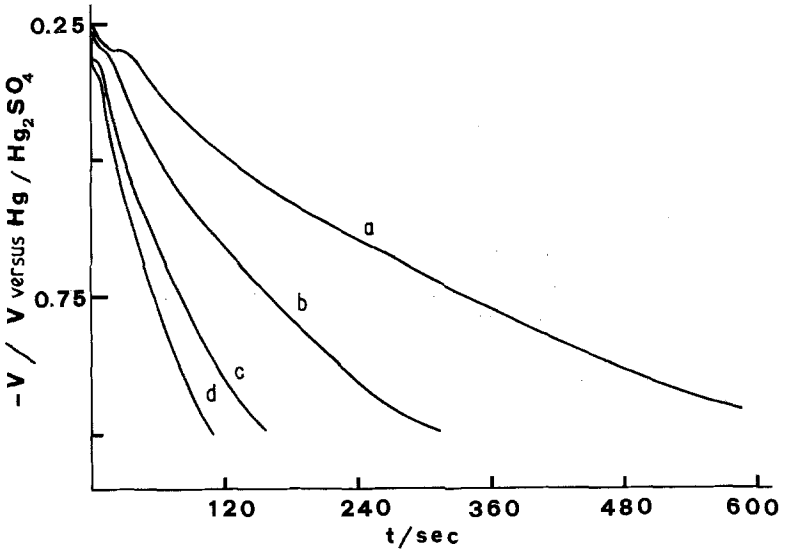

Fig. 1. Dependence of electrode potential on time: (a) $i = 12.5\,\mu A\,cm^{-2}$; (b) $i = 25\,\mu A\,cm^{-2}$; (c) $i = 50\,\mu A\,cm^{-2}$; (d) $i = 75\,\mu A\,cm^{-2}$.

delocalization of the trapped electrons and therefore the absence of a close spatial correlation [21, 25].

Some comment is necessary about the electrode potential values reported in Fig. 2. In Equation 6 the reversible electrode potential should be used. Instead the V values include both the ohmic drop within the electrode and the electrode process overvoltage. Both contributions affect the measured electrode potential in an unpredictable way, because the composition of the electrode changes continuously during the coloration. However if we take into account the small current densities employed we can suppose that both contributions are negligible after the initial stage of coloration [18, 26]. This is in agreement with the initial shift from the straight-line behaviour. This shift also increases with the current density. At very cathodic electrode potentials the shift from the straight line can be attributed to the start of hydrogen evolution which decreases the efficiency of vacancy injection.

3.2. *Potentiostatic measurements*

A check of the diffusion model previously discussed was carried out by potentiostatic experiments. The electrode potential was controlled between -0.40 V and -0.55 V with respect to the reference electrode, so to avoid the competing hydrogen evolution process.

In Figs. 3 and 4 typical plots of i versus t are shown for two different electrode potentials. The solid lines are the pen-recorded curves while the solid circles are the theoretical points obtained solving the time-dependent Fick's equation with

Table 1. Surface vacancy concentrations x (moles of vacancies)/(moles of $WO_3 \cdot H_2O$*) obtained by Equation 5 at different current densities as a function of the electrode potential V*

V (V versus Hg/Hg_2SO_4)	x			
	$12.5\,\mu A\,cm^{-2}$	$25\,\mu A\,cm^{-2}$	$50\,\mu A\,cm^{-2}$	$75\,\mu A\,cm^{-2}$
−0.30	0.0079	0.0074	0.0012	0.0011
−0.35	0.0136	0.0133	0.0121	0.0123
−0.40	0.0188	0.0185	0.0179	0.0183
−0.45	0.0246	0.0240	0.0237	0.0243
−0.50	0.0314	0.0305	0.0303	0.0308
−0.55	0.0400	0.0385	0.0378	0.0389

suitable conditions [27]. The main assumption made to solve the Fick's Equation concerns the time-dependence of the surface vacancy concentration:

$$c = c_0[1 - \exp(-t/\tau)] \quad (7)$$

where c_0 is the final concentration which is assumed equal to the value reported in Table 1 for the different electrode potentials. The time constant τ gives the rate of increase of c at each applied potential [14]. Then for each experiment τ is obtained by the best fitting of Equation 8 to the data. The final expression for the current density is

$$i = zFDc_0 \exp(-t/\tau)\left(\frac{1}{D\tau}\right)^{1/2} \tan\left[l\left(\frac{1}{D\tau}\right)^{1/2}\right] + zFDc_0 \frac{16l^2}{\pi\tau} \sum_{n=0}^{\infty} \frac{\pi}{2l} \times \frac{(-1)^n \exp[-D(2n+1)^2\pi^2 t/(4l^2)]}{[4l^2/\tau - D\pi^2(2n+1)^2]} \times \sin\frac{(2n+1)\pi}{2} \quad (8)$$

The data employed in Equation 8 to obtain the theoretical points are shown in Table 2. The fitting of the experimental curves is performed with the D value previously reported (see Section 3.1). Good fitting is found between experimental and theoretical curves except at short times, when other factors seem to control the rate of the process.

The transport of H^+ through the electrode–electrolyte interface could be the r.d.s. in this region [14], but a check of this hypothesis would require a knowledge both of the exchange current density and the symmetry factor, as functions of the variable surface concentration [26].

In Fig. 5 is reported a plot of i versus $t^{-1/2}$. It is noteworthy that at longer times the current deviates from the $t^{-1/2}$ line, although the good fit of theoretical to experimental data confirms that the diffusion mechanism is always operating.

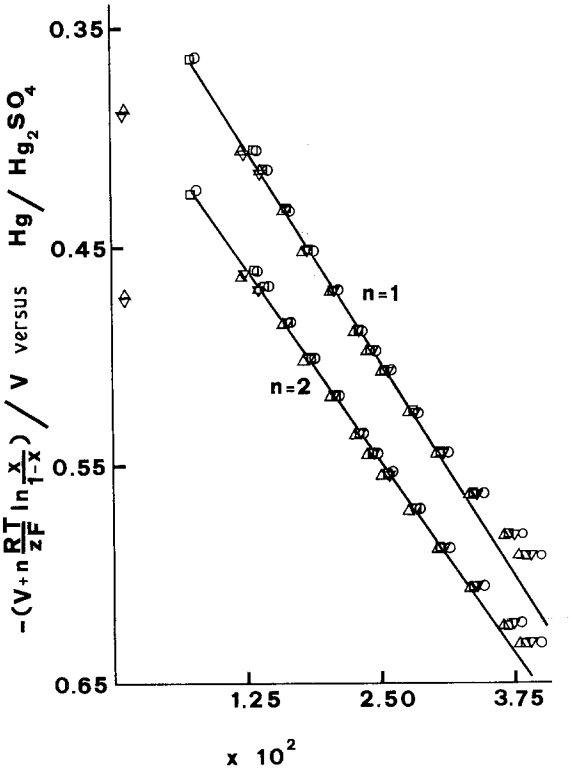

Fig. 2. Plot of $V + n[RT/(zF)] \ln[x/(1-x)]$ versus vacancy concentration: $\circ i = 12.5\,\mu A\,cm^{-2}$; $\square i = 25\,\mu A\,cm^{-2}$; $\triangle i = 50\,\mu A\,cm^{-2}$; $\triangledown i = 75\,\mu A\,cm^{-2}$.

4. Conclusions

On the basis of the experimental results the coloration process of anodic $WO_3 \cdot H_2O$ layers seems to be governed by a vacancy diffusion process after an initial stage during which a barrier-limited proton transport across the oxide–electrolyte interface could be the r.d.s.

Table 2. Data employed for solving Equation 8, at different applied electrode potentials

V (V versus Hg/Hg_2SO_4)	l (μm)	τ (s)	x_0 (*moles of vacancies*)/(*moles of* $WO_3 \cdot H_2O$)
−0.40	0.1170	1.56	0.0185
−0.45	0.1037	0.71	0.0242
−0.50	0.1025	0.57	0.0306
−0.55	0.1095	0.53	0.0385

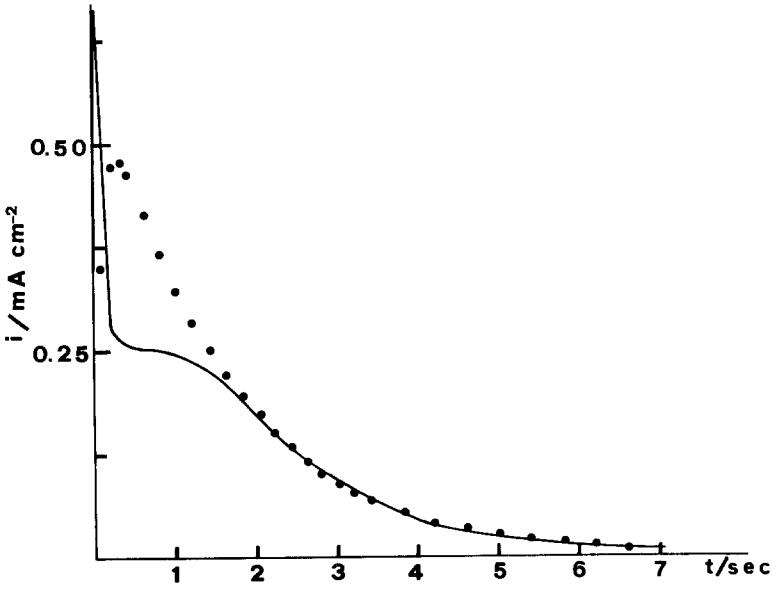

Fig. 3. Dependence of colouring current on time for $V = -0.4$ V. The solid curve is experimental, the dotted curve is theoretical.

In this picture the appearance of an inflection point both on the V versus t curves at constant current and on the i versus t curves at a fixed electrode potential, would support the transition from a barrier controlled process to a vacancy diffusion controlled process.

The hypothesis of a surface vacancy concentration as the electrode potential determining parameter is in agreement with the experimental results.

Indeed from the D value, an activation energy for the diffusion process is about 0.35 eV. This is a reasonable value for a solid state vacancy diffusion process and represents a further proof of the previously proposed mechanism.

As for the amount of electric charge circulated during the coloration process, it is worthwhile to note that about 60% of the total circulated charge in a potentiostatic experiment is spent when a vacancy diffusion control is operating. This sets

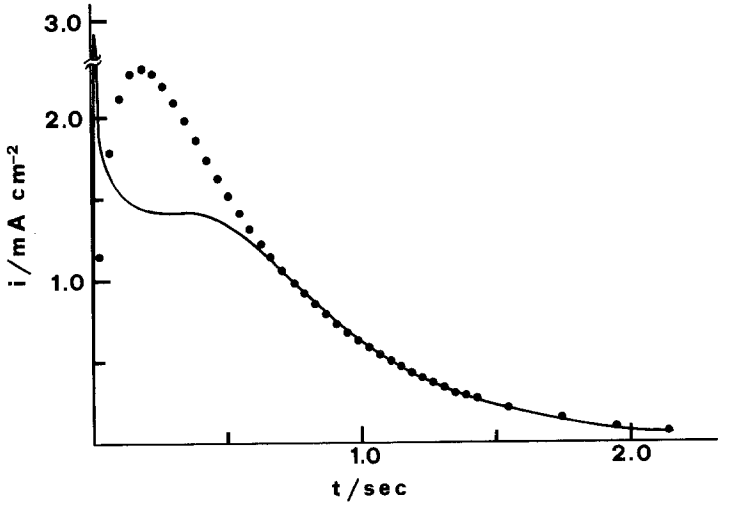

Fig. 4. Dependence of colouring current on time for $V = -0.55$ V. The solid curve is experimental, the dotted curve is theoretical.

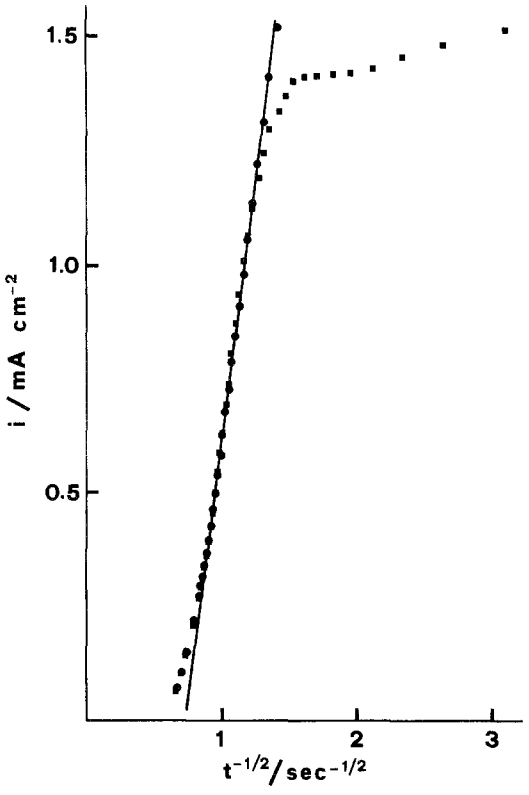

Fig. 5. Coloration current versus $t^{-1/2}$, for $V = -0.55$ V. The circles are theoretical points obtained using Equation 8, the squares are experimental values.

some limits to the possible coloration rates especially if a deep coloration is required. Moreover the potentiostatic measurements show that the colouring response time of $WO_3 \cdot H_2O$ electrochromic films is always longer than 0.5 s which is the optimum time response of a display device [18].

Therefore at potentials at which side reactions should be absent the colouring rate of $WO_3 \cdot H_2O$ anodic films seems unsatisfactory for practical display devices. Further investigations at higher potentials seem necessary for a more complete evaluation of their applicability. It will be recalled, however, that the bleaching process occurs more easily in $WO_{3-x} \cdot H_2O$ electrochromic layers than in hydrogen tungsten bronzes [12].

Acknowledgements

The financial support of the CNR Technological Committee (Rome) is gratefully acknowledged.

References

[1] J. Kirton, H. R. Zeller, I. F. Chang, G. E. Weibel and J. Bruinink in 'Non emissive electrooptic displays' (edited by A. R. Kmetz and F. K. von Willisen) Plenum Press, London (1976).
[2] M. L. Hitchman, *J. Electroanalyt. Chem.* **85** (1977) 135.
[3] E. K. Sichel, J. I. Gittleman and J. Zelez, *Appl. Phys. Lett.* **31** (1977) 109.
[4] T. J. Knowles, *Appl. Phys. Lett.* **31** (1977) 817.
[5] S. K. Mohapatra and S. Wagner, *J. Electrochem. Soc.* **125** (1978) 1603.
[6] J. P. Randin, *J. Elect. Mater.* 7 (1978) 47.
[7] A. Deneuville and P. Gerard, *ibid* 7 (1978) 559.
[8] S. K. Mohapatra, G. D. Boyd, F. G. Storz, S. Wagner and F. Wudl, *J. Electrochem. Soc.* **126** (1979) 805.
[9] B. W. Faughnan, R. S. Crandall and P. M. Heyman, *RCA Review* **36** (1975) 177.
[10] O. F. Schirmer, V. Wittwer, G. Bauer and G. Brandt, *J. Electrochem. Soc.* **124** (1977) 749.
[11] W. C. Dautremont-Smith, M. Green and K. S. Kang, *Electrochim. Acta* **22** (1977) 751.
[12] A. Di Paola, F. Di Quarto and C. Sunseri, *J. Electrochem. Soc.* **125** (1978) 1344.
[13] G. Elliott, *The Radio and Electronic Engineer* **46** (1976) 281.
[14] R. S. Crandall and B. W. Faughnan, *Appl. Phys. Lett.* **28** (1976) 95.
[15] S. K. Mohapatra, *J. Electrochem. Soc.* **125** (1978) 284.
[16] I. F. Chang, B. L. Gilbert and T. I. Sun, *ibid* **122** (1975) 955.
[17] B. Reichman and A. J. Bard, *ibid* **126** (1979) 583.
[18] M. Green, W. C. Smith and J. A. Weimer, *Thin Solid Films* **38** (1976) 89.
[19] 'Handbook of Chemistry and Physics', 56th ed., C.R.C. Press, Cleveland, Ohio (1975–76).
[20] A. Di Paola, F. Di Quarto and C. Sunseri, *Corr. Sci.* to be published.
[21] M. J. Sienko and J. M. Berak, in 'The Chemistry of extended defects in non metallic solids' (edited by L. R. Eyring and M. O'Keeffe) North Holland Publishing Co., Amsterdam (1970) p. 541.
[22] R. Hurditch, *Electron. Lett.* **11** (1975) 142.
[23] H. S. Carlslaw and J. C. Jaeger, 'Conduction of heat in solids' 2nd ed., Oxford University Press, Oxford (1959) p. 112.
[24] R. S. Crandall, P. J. Wojtowicz and B. W. Faughnan, *Solid State Commun.* **18** (1976) 1409.
[25] N. F. Mott and R. W. Gurney, 'Electronic processes in ionic crystals' 2nd ed., Dover Publications Inc., New York (1964) p. 109.
[26] T. C. Arnoldussen, presented at *The Electrochemical Society Meeting*, Las Vegas, Nevada, October (1976) – paper 199.
[27] J. Crank, 'The Mathematics of Diffusion', 2nd ed., Clarendon Press, Oxford (1975) pp. 53, 62.